Analytical Methods

ROYAL SOCIETY OF CHEMISTRY

PAPER

View Article Online
View Journal | View Issue

Check for updates

Cite this: *Anal. Methods*, 2025, **17**, 5062

Non-invasive Raman spectroscopy for monitoring metabolite changes in tomato plants infected by phytoplasma†

Lorenzo Pandolfi, ‡[ac] Niccolò Miotti, ‡[b] Guido Faglia, [c] Carlo Pennacchio, [a] Andrea Ponzoni, [a] Marina Ciuffo, [b] Sabrina Palmano, [b] Martino Schillaci, [b] Emanuela Gobbi, [d] Massimo Turina [b] and Camilla Baratto *[a]

The increasing demand for food production requires innovative approaches to protect crops from pathogens that significantly reduce yield and quality. Phytoplasmas, persistent bacterial pathogens transmitted by phloem-feeding insects, cause severe damage to economically important crops, including tomato plants. Early detection of these pathogens can be crucial considering that traditional molecular diagnostic methods, such as polymerase chain reaction (PCR), often fail during early infection stages due to low pathogen concentrations. In this study, we explore the use of Raman spectroscopy as a rapid, non-invasive tool for monitoring alterations in plant metabolites caused by *Candidatus* Phytoplasma solani infection in tomato plants. Grafting experiments were performed, and Raman spectra were collected at different time intervals post-infection. Changes in the spectral intensities of chlorophyll, carotenoids, and polyphenols were identified as early as two weeks post-infection, prior to the pathogen's detectability by molecular methods. These findings highlight the potential of Raman spectroscopy to fill the diagnostic gap in the early stages of phytoplasma infections, offering a window for timely intervention and a further tool in precision agriculture.

Received 21st February 2025
Accepted 19th May 2025

DOI: 10.1039/d5ay00293a

rsc.li/methods

Open Access Article. Published on 20 May 2025. Downloaded on 9/10/2025 12:20:14 PM.
This article is licensed under a Creative Commons Attribution 3.0 Unported Licence.

Introduction

World population and global food demand are rapidly growing, creating the need for an efficient production system. One of the main concerns is plant pathogens, which still affect the yield and quality of agricultural products, compromising crops and causing severe economic losses.[1,2] Hence, pest management based on expensive agrochemicals is necessary in the modern agricultural industry, when preventive strategies fail. However, widespread usage of these crop-protection products may raise serious issues for food safety and the environment.[3] Early and timely detection of pathogens in diseased plant material is one potential remedy, which would enable the effective use of agrochemicals with specific targeting of interventions and timely administration to limit epidemics. This approach falls generally under the so-called "precision agriculture", a protocol of tailored agricultural practices applied only when and where they are really needed, for more sustainable farming.[1,4,5] However, since the first stages of many pathogen infections are symptomless (latency), it is difficult to just rely on visual symptom observation for early monitoring of infections. In many cases, interventions based on symptoms can frequently be too late to prevent significant economic losses. This is particularly true when dealing with pathogens (like phytoplasmas) characterized by persistent infections, for which no direct therapy in the field is available. In some cases, even refined and sensitive molecular analyses, such as polymerase chain reaction (PCR) or serological assays, fail to detect the pathogen systemically in a newly infected organism since its concentration can be below the limit of detection (LOD). In this context, the early detection of phytoplasmas can significantly reduce yield losses and the spread of this pathogen in the environment.

Phytoplasmas are obligate bacteria restricted to the phloem and classified under the Mollicutes class. They are transmitted by phloem-feeding insects (Hemiptera) due to their *trans*-kingdom capability to invade and replicate within both plant and animal cells.[6] These pathogens are linked to diseases that affect hundreds of plant species, including several economically important crops and fruit trees.[7] Among these, tomato plants (*Solanum lycopersicum* L.) host several phytoplasmas worldwide

[a]*National Research Council – National Institute of Optics (CNR-INO), Via Branze 45, 25123 Brescia, Italy. E-mail: camilla.baratto@cnr.it*

[b]*National Research Council – Institute for Sustainable Plant Protection (CNR-IPSP), Strada delle Cacce 73, 10135 Turin, Italy*

[c]*Department of Information Engineering – University of Brescia, Via Branze 38, 25123 Brescia, Italy*

[d]*Department of Molecular and Translational Medicine – University of Brescia, Viale Europa 11, 25123 Brescia, Italy*

† Electronic supplementary information (ESI) available. See DOI: https://doi.org/10.1039/d5ay00293a

‡ These authors contributed equally to this work.

This journal is © The Royal Society of Chemistry 2025

Open Access Article. Published on 20 May 2025. Downloaded on 9/10/2025 12:20:14 PM. This article is licensed under a Creative Commons Attribution 3.0 Unported Licence.

but one of the most economically relevant is the *Candidatus* Phytoplasma solani (*Ca.* P. solani).[8] *Ca.* P. solani, formerly referred to as "stolbur phytoplasma", affects different agricultural crops across Europe with considerable damage to numerous economically valuable plants and significantly compromises tomato production since fruits from the infected plants cannot be harvested and marketed.[9]

An alternative to direct detection of pathogens can be the monitoring of chemical changes occurring in plant metabolites after infection. In this context, chromatographic techniques, such as high-performance liquid chromatography (HPLC) or gas chromatography (GC), have so far represented the gold-standard analyses in the separation and analyte detection due to their high precision. However, costly instrumentation, time-consuming sample preparation and qualified operators still represent the major drawbacks of these methods.[3,10] Recently, to get over these limitations, Raman spectroscopy has been applied as a technique for early identification of plant diseases and abiotic stresses.[1,11–14] In particular, the recent development of portable Raman devices allowed the broadening of the investigation from the laboratory scale to in-field analysis.[15–22] Hand-held Raman devices allow for fast and non-destructive *in situ* measurements of biotic and abiotic stress responses of plant tissue.[1,5] The operation involves the direct comparison of the Raman pattern of a diseased sample *vs.* that of the control specimen; as signal variations are very limited, the use of multivariate analysis along with statistical approaches is needed.[11,16–22] Up to date, hand-held Raman devices have been utilized for the early detection of plant viruses and bacteria in green-leaf plants,[13–15,18,20] fungal infections in wheat grains[16,19] and maize kernels,[17] as well as characterization of abiotic stresses.[21]

The following study aims to investigate the use of Raman spectroscopy for the evaluation of alterations in experimentally grafted infected tomato plants with phytoplasma. To the best of our knowledge, this is the first application of Raman spectroscopy to characterize the effects of phytoplasma infections in plants.

Experimental

Plant material and phytoplasma strain

The *Ca.* P. solani strain used in this study was originally isolated from an infected tomato from Foggia and maintained *in vivo* at the Institute of Sustainable Plant Protection (IPSP) phytoplasma collection by grafting onto tomato plants cv. Marmande.[23] Several tomatoes were inoculated in advance to provide sufficient numbers of infected scions for the grafting procedures used in the experiments. For the experiments, every two weeks, three plants were grafted with infected plant material and three other plants were grafted with healthy scions to act as a negative control. Biweekly grafts were performed in the stem at the level of the first true leaf, for a total of 24 plants over two months. The grafted plants have been grown in the greenhouse of the IPSP (Turin, Italy) in a controlled environment (16/8-hour day/night photoperiod, 25 °C and 18 °C day/night temperatures, and 70% relative humidity).

Raman spectroscopy

The Rigaku Progeny hand-held spectrometer has been utilized for the Raman analysis. The device features a source wavelength of 1064 nm, a laser spot size of 25 μm, an adjustable laser power (30–490 mW) and a spectral resolution of about 8–11 cm^{-1}. The TE cooled InGaAS 512-pixel detector allows for high resolution measurements, with the acquisition range spanning from 200 cm^{-1} to 2500 cm^{-1}. For Raman measurements, an acquisition time of 5 seconds with 1 accumulation has been chosen, with a laser power of 450 mW, which provided the optimum compromise between signal intensity and leaflet damage. In order to have a flat surface and reduce the stray light, a metal plaque has been used to gently press the analysed leaflet against the focus nose cone, for *in situ* measurement. 24 tomato plants were analysed (6 for each graft). Three to four leaflets per plant have been measured, whilst on each leaflet two to three spectra were recorded. Leaflets with similar maturity were chosen. The total number of recorded Raman spectra was 154. For each experimental spectrum acquired, a baseline subtraction of the raw data has been applied using the asymmetric least squares (ALS) method. Then, the subtracted spectrum has been normalised by the integrated area, in order to exclude external physical parameters (*e.g.*, laser power, acquisition time, *etc.*).

Chemometrics. Partial least squares discriminant analysis (PLS-DA) was conducted using the Classification toolbox of MATLAB®, a collection of MATLAB® modules for classification (supervised pattern recognition) through multivariate models.[24] Raw spectra were extracted in the range 700–1700 cm^{-1} and preprocessed by Savitsky–Golay smoothing (11 points, polynomial order 3), removing random shift of the baseline offset by asymmetric least-squares (ALS) baseline correction.[25,26] Data were normalised by the integrated area and the output variables were categorical either healthy or infected. Samples were assigned to the class with maximum probability. The number of latent variables was set to five, after error minimization through cross validation. Two healthy and three infected plants were randomly selected for testing, leaving the others for training; this process was repeated one thousand times to get meaningful (mediated) results. The Variable Importance in the Projection (VIP) scores for the PLS model applied to the data were the weighted sum of squares of the PLS weights, reflecting the amount of explained by variance in each extracted latent variable.[27] Principal component analysis (PCA) was performed adopting the embedded toolbox of OriginPro® 2018. Raw spectra were preprocessed by asymmetric least-squares (ALS) baseline correction and normalised by the integrated area. Each spectral peak was fitted with a Gaussian curve and utilized as an input feature for the multivariate analysis. The loading plot was used to interpret relationships between variables.

Molecular analysis for the detection of *Ca.* P. solani

Leaflets were sampled, after the Raman measurement, and stored at −20 °C in an extraction bag (BIOREBA). Detection of *Ca.* P. solani was carried out using two distinct molecular analyses. The first method employed qPCR with universal primers for phytoplasma CY2, as described by Galletto *et al.*

Open Access Article. Published on 20 May 2025. Downloaded on 9/10/2025 12:20:14 PM.
This article is licensed under a Creative Commons Attribution 3.0 Unported Licence.

2005.[28] Relative quantification of the pathogen titer, as genome units (GUs) per ng of DNA extracted, was calculated following the protocol outlined by Marzachì *et al.* 2005.[29] Reactions were performed using SYBR™ Green Universal Master Mix (Applied Biosystems™) according to the manufacturer's instructions. The second method was based on a one-step RT-qPCR, conducted on crude extracts according to the procedure described by Margaria *et al.* (2009).[30,31] M-MLV Reverse Transcriptase (Thermo Fisher Scientific) was used for the reverse transcription step, while iTaq Universal Probes Supermix (Bio-Rad) was employed for the PCR reactions, following the manufacturers' guidelines.

Statistical analysis. Before assessing the statistical significance of differences between calculated GUs, data normality and variance homogeneity were tested with the Shapiro–Wilk test and Levene's test, respectively. The effect of the categorical independent variable "time" on GU per ng was evaluated with a one-way ANOVA.

Results and discussion

The Raman spectrum of a green leaflet

All experimental spectra have been displayed in Fig. 1, blue lines corresponding to mock-grafted (healthy) plants and red lines to infected plants. It appears clear that no additional vibrational mode associated with inoculated plants arises from the Raman pattern, representing a unique marker of the pathogen. The straightforward difference lies in the diverse intensity ratios of some peaks, especially at higher frequencies (1500–1600 cm^{-1}). The nature of these peaks can be revealed with a thorough vibrational analysis in the literature. The vibrational assignment of the Raman spectrum of a green leaf has been already achieved by previous studies.[13,15,18,20,22] However, this aspect is not fully investigated yet, since major contradictions still exist in the vibrational assignment even for the most intense modes, as illustrated in Table 1. Nonetheless, arguably some reference vibrations which correspond to specific chemical families can be identified. Among the most intense bands, modes at 1005, 1187, 1212 and 1525 cm^{-1} belong to the chemical family of carotenoids. The frequency peaking at 1326 cm^{-1} correspond to the family of chlorophylls. Finally, the vibration at 1604 cm^{-1} correlates with the class of polyphenols.

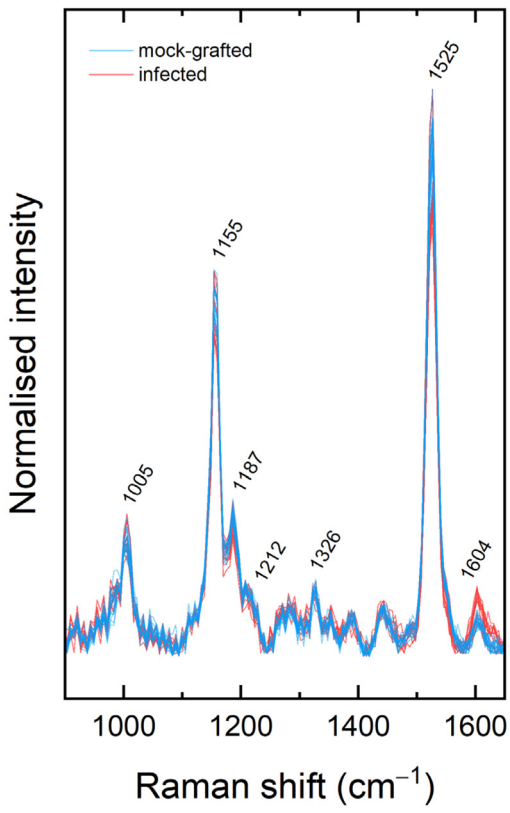

Fig. 1 All experimental Raman spectra from tomato plants, displayed from 900 cm^{-1} to 1650 cm^{-1}. Mock-grafted (blue lines) and infected plants (red lines) are shown.

Evaluation of infection by Raman spectroscopy

The entire spectral database has been evaluated by means of multivariate analysis. In fact, the partial least squares (PLS) regression algorithm allowed the identification of the most relevant peaks among the entire spectrum. These modes are displayed in the variable importance plot (VIP) of Fig. S1 (ESI).† Based upon the results of the VIP, three vibrational modes were selected, which are plotted in Fig. 2. The first frequency lies at 1326 cm^{-1} (ν_1), representing one of the few modes which can be ascribed solely to chlorophyll; the second peak is at 1525 cm^{-1} (ν_2), the most intense Raman band of the spectrum, attributed to the chemical family of carotenoids; the last one falls at 1604 cm^{-1} (ν_3), belonging to the class of polyphenols. These vibrations were selected since they also guarantee no overlap between the spectral features of different chemical families. Furthermore, to verify that the three chosen modes were not intrinsically correlated, each band was fitted with a Gaussian curve, and the peak intensity, *i.e.*, the area under the curve, was utilized as the input feature for principal component analysis (PCA). Consequently, the intensities of the three selected vibrations have been box-plotted by metabolite type for each group of plants. The data acquired at two, four, six and eight weeks post-grafting (2 wpg, 4 wpg, 6 wpg and 8 wpg, respectively) were analysed. In Fig. 3, the results for the set of plants which have been grafted for two weeks (2 wpg) are displayed. Comparing the box-plot of infected (group A) and control (group B) plants, the content of chlorophyll appears to be similar (mean difference of 2%), while diverse carotenoid and polyphenol contents is highlighted. In particular, after the infection, the mean value for carotenoid content is lower than the control plants by 7.5%, while average polyphenol content increased by 46%. The set of plants which have been grafted for four weeks (4 wpg) shows diverse metabolite contents compared to the control plants, as displayed in Fig. 4. Specifically, the average chlorophyll content increased by 7% and the mean value of carotenoid content was lower than that of control plants by 5%, while polyphenol content increased by 27%. Measurements have been performed also with plants which have been grafted for 6 weeks (6 wpg) and 8 weeks (8 wpg);

 This journal is © The Royal Society of Chemistry 2025

Open Access Article. Published on 20 May 2025. Downloaded on 9/10/2025 12:20:14 PM. This article is licensed under a Creative Commons Attribution 3.0 Unported Licence.

Table 1 Literature vibrational assignments of Raman modes in a green leaf sample

ν (cm^{-1})	Yeturu *et al.* 2016 (ref. 15)	Mandrile *et al.* 2019 (ref. 13)	Sanchez *et al.* 2020 (ref. 20)
915	chlorophyll	chlorophyll	cellulose, lignin
1004	carotenoids	carotenoids	carotenoids, protein
1155	carotenoids	carotenoids	carbohydrates, cellulose
1187	carotenoids	chlorophyll	xylan
1212	carotenoids	chlorophyll	aliphatic
1326	carotenoids	chlorophyll	cellulose, lignin
1525	carotenoids	carotenoids	carotenoids
1604	lignin	lignin, polyphenolics	lignin, proteins

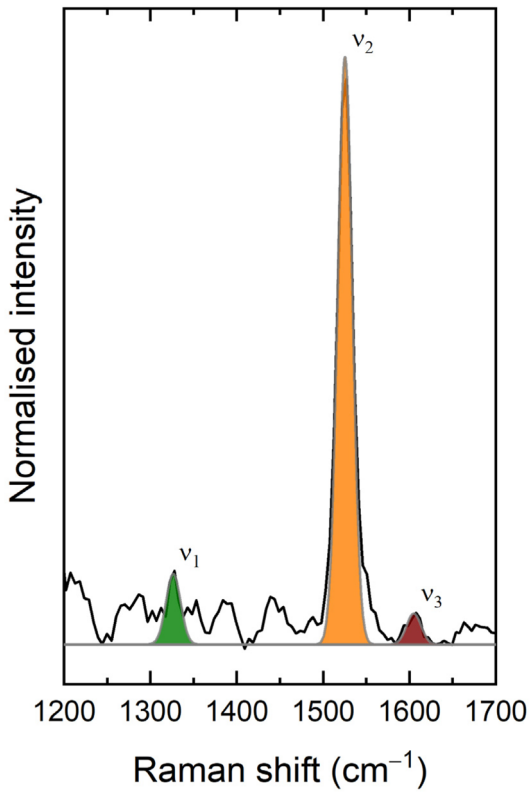

Fig. 2 For each spectrum, peak fitting has been performed. The vibration at 1326 cm^{-1} (ν_1) has been chosen to represent the chlorophyll content and the band at 1525 cm^{-1} (ν_2) describes the carotenoid content, while the polyphenol content is indicated by the peak at 1604 cm^{-1} (ν_3).

however, the box-plots do not show relevant differences (Fig. S2 and S3 respectively, shown in the ESI†).

Detection of phytoplasma infections using molecular analyses

The detection of *Ca.* P. solani using the first qPCR methodology successfully identified and quantified pathogen GUs in leaflets sampled from plants at 4 wpg, 6 wpg, and 8 wpg, as depicted in Fig. 5. However, no GUs were detected in leaflets sampled from 2 wpg plants. Statistical analyses confirmed that, despite the increasing trend of bacterial titre through time, no significant differences were found among the three sampling dates where the presence of phytoplasma could be detected. (Table S1†). Similar results were obtained using a second molecular analysis based on a fast crude-sap based one-step RT-qPCR protocol, where no signal was detected in the 2 wpg leaflet samples (Table S2, ESI†).

Discussion

Phytoplasma-infected plants commonly show a range of symptoms, including abnormal proliferation of auxiliary buds (witches' brooms), morphological changes in floral organs (phyllody and virescence), leaf chlorosis (yellowing) and curling, flower malformation and sterility (Fig. S4†). In infected tomatoes, these symptoms generally do not appear until 4–6 weeks after infection, a delay that makes disease control difficult. For this reason, a sensitive molecular diagnostic method such as real-time PCR is used, but in our experiments it failed to detect systemic infection at 2 weeks after grafting. Therefore, inspecting plant metabolites using non-destructive techniques such as Raman spectroscopy can be a reliable alternative, providing guidance for more precise pathogen-detection analyses. Since phytoplasmas lack key metabolic genes required for independent survival,[32] their infection creates an interconnected metabolic network between the pathogen and its host,[33] as both compete for the same nutrients within the plant, leading to modulation of photosynthesis,[34–36] flavonoid biosynthetic pathways,[37] defense-related genes and hormone-signaling pathway.[38] Consistent with these previous studies on phytoplasma infected plants, in the present work, the Raman investigation showed differences in chlorophyll, carotenoid and polyphenol content between infected and mock-grafted tomatoes at 2 wpg and 4 wpg (Fig. 3 and 4). Alongside this, both molecular analyses failed to detect the pathogen in plants at 2 wpg (Fig. 5), suggesting that the differences in metabolite concentrations observed *via* Raman spectroscopy may reflect early signalling events triggered by the infection, even in the absence of detectable pathogen DNA or RNA in the sampled

Open Access Article. Published on 20 May 2025. Downloaded on 9/10/2025 12:20:14 PM.
This article is licensed under a Creative Commons Attribution 3.0 Unported Licence.

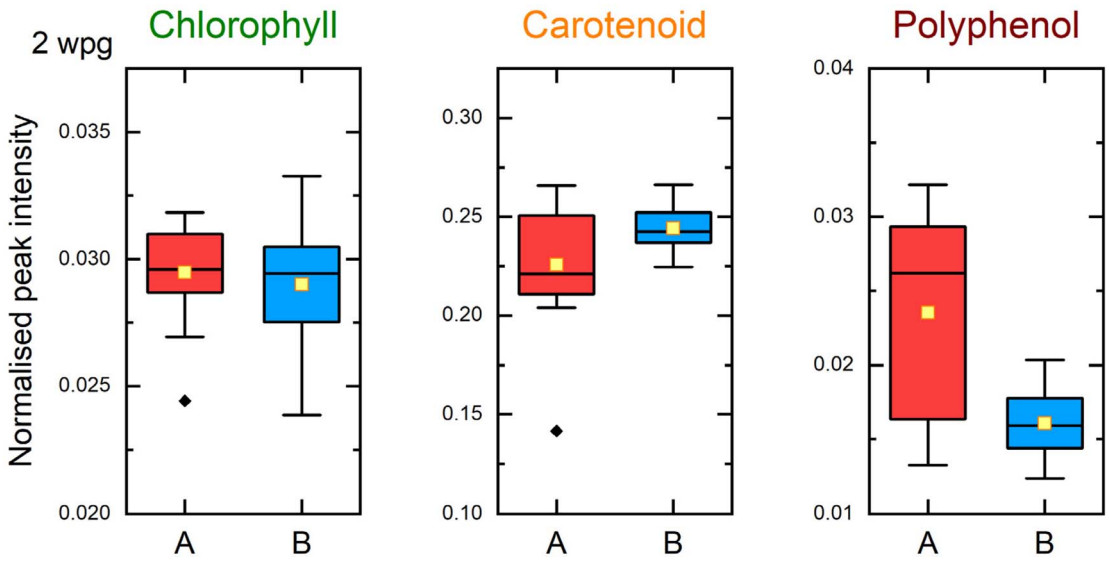

Fig. 3 Box-plot of the intensities of v_1 (chlorophyll), v_2 (carotenoid) and v_3 (polyphenol) from group A (infected plants) and group B (control plants). Plants have been grafted for two weeks (2 wpg). Mean values are depicted by a yellow square, while the median is denoted by a straight line. Average chlorophyll content seems constant, comparing infected and mock plants. Mean carotenoid content decreases for infected plants, while polyphenol content increases. (Black diamonds are outliers).

leaflets. This suggests that Raman spectroscopy holds promise for the early detection of infection-induced alterations in metabolite content. In fact, the possibility that the grafting process alone, or any other abiotic stress (*e.g.*, natural senescence),[39] caused these alterations is excluded, as grafts using healthy material did not exhibit significant differences in metabolite levels. These findings underscore the potential of Raman spectroscopy to identify early biochemical responses in plants during phytoplasma infection. However, it is important to note that changes in pigment levels detected by Raman spectroscopy are not currently specific to phytoplasma infections, since similar alterations have been observed for viruses[15] and abiotic stresses.[12]

Following experiments will be dedicated to investigating the time frame from one to four weeks post-grafting, with the aim of precisely identifying the moment when Raman spectroscopy could detect variations in metabolite content and when the pathogen would reach the analysed leaflet, making it detectable by means of molecular analyses. Future studies should also explore the biochemical responses of tomato plants under

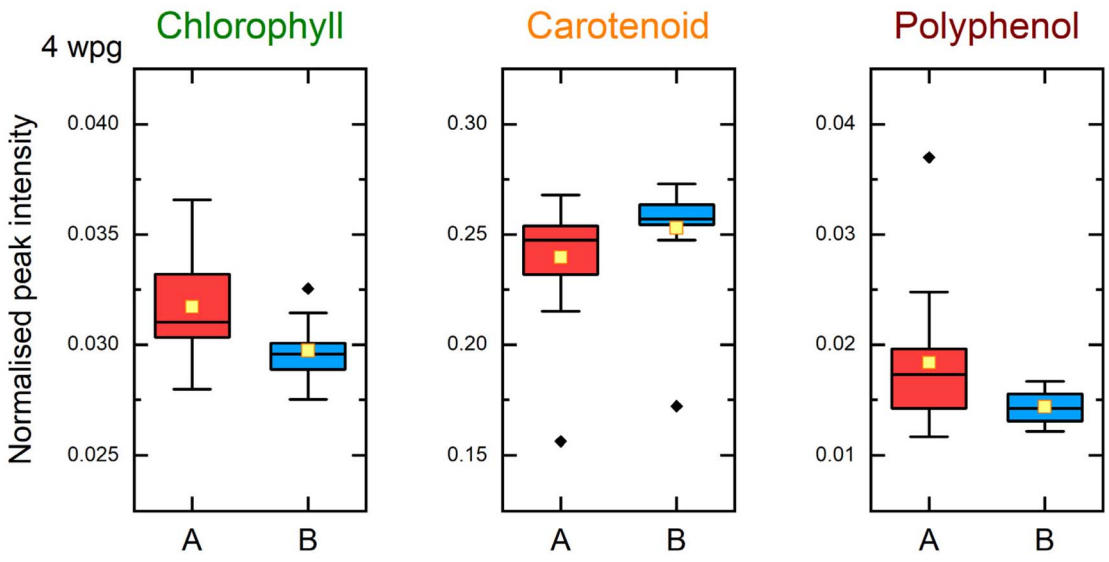

Fig. 4 Box-plot of the intensities of v_1 (chlorophyll), v_2 (carotenoid) and v_3 (polyphenol) from group A (infected plants) and group B (control plants). Plants have been grafted for four weeks (4 wpg). Box-plot mean values are depicted by a yellow square, while the median is denoted by a straight line. Average chlorophyll content is increased in infected plants. Mean carotenoid content decreases for infected plants, while polyphenol content increases. (Black diamonds are outliers).

 This journal is © The Royal Society of Chemistry 2025

Open Access Article. Published on 20 May 2025. Downloaded on 9/10/2025 12:20:14 PM.
This article is licensed under a Creative Commons Attribution 3.0 Unported Licence.

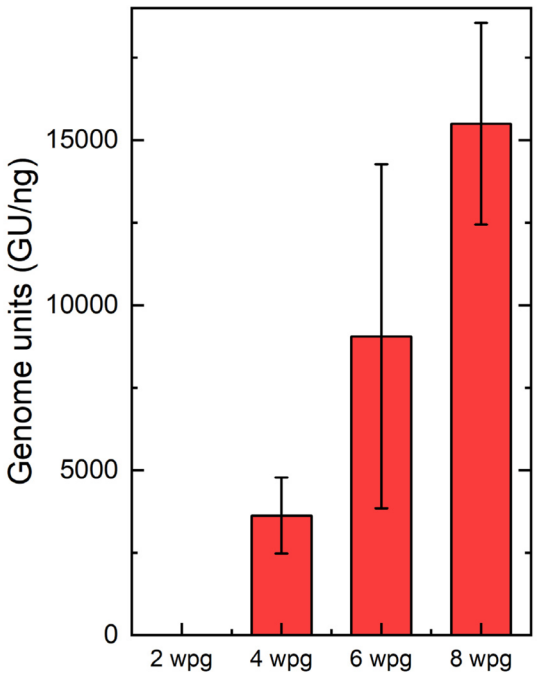

Fig. 5 Barplot displaying the relative quantification of *Ca*. P. solani, expressed in genome units (GU) per ng of total DNA extracted from infected tomatoes at different time points of the experiment. No trace of phytoplasma GU was detected in plants after two weeks post-grafting (2 wpg). Bars display the mean ± standard error, with three biological replicates at all time points.

various stress conditions, both biotic and abiotic, to determine whether a specific marker can be reliably associated with phytoplasma infections.

Conclusions

Raman spectroscopy can detect significant metabolic alterations indicative of underlying stress induced by *Ca.* P. solani infection. While the pathogen cannot be specifically diagnosed, we demonstrated that the observed alterations are detectable earlier (2 wpg) than the quantification by means of q-PCR, which is possible only after four weeks (4 wpg). This approach can act as an early warning signal, particularly in intensive production environments such as nurseries and greenhouses, triggering further analyses to confirm the presence of possible infection and enabling a rapid disease containment system to be activated. Another notable aspect of this study is the methodology presented. This protocol achieves the simultaneous evaluation of three key metabolites (*i.e.*, chlorophyll, carotenoids, and polyphenols) in a non-destructive and rapid manner, without the need for demanding multivariate analyses, making it easily transferable to monitoring plant physiological responses.

Data availability

The data supporting this article have been included as part of the ESI.†

Author contributions

L. Pandolfi: conceptualization, investigation, methodology, formal analysis, and writing; N. Miotti: conceptualization, investigation, methodology, and writing; G. Faglia: formal analysis and software; C. Pennacchio: formal analysis, software, and writing; A. Ponzoni: conceptualization; M. Ciuffo: conceptualization and methodology; S. Palmano: conceptualization, methodology, and writing; M. Schillaci: investigation and methodology; E. Gobbi: conceptualization; M. Turina: conceptualization, methodology, project administration, and supervision; C. Baratto: conceptualization, methodology, project administration, and supervision.

Conflicts of interest

There are no conflicts to declare.

Acknowledgements

This study was supported by European Union-Next Generation EU M4C2 1.1 under Grant PRIN 2022JZAA9W–SENSEPLANET and by the "Agritech National Research Center" funded by the European Union Next-Generation EU (Piano Nazionale di Ripresa e Resilienza (PNRR) – Missione 4 Componente 2, Investimento 1.4 – D.D. 1032 17/06/2022, CN00000022).

Notes and references

1 P. J. Chung, G. P. Singh, C.-H. Huang, S. Koyyappurath, J. S. Seo, H.-Z. Mao, P. Diloknawarit, R. J. Ram, R. Sarojam and N.-H. Chua, *Front. Plant Sci.*, 2021, **12**, 746586.
2 S. Weng, X. Hu, J. Wang, L. Tang, P. Li, S. Zheng, L. Zheng, L. Huang and Z. Xin, *J. Agric. Food Chem.*, 2021, **69**, 2950.
3 Y. Jiang, D. Sun, H. Pu and Q. Wei, *Trends Food Sci. Technol.*, 2018, **75**, 10.
4 W. S. Lee and R. Ehsani, *Comput. Electron. Agric.*, 2015, **112**, 2.
5 M. Roy and A. Prasad, *Materialia*, 2022, **24**, 101474.
6 S. A. Hogenhout, K. Oshima, E. D. Ammar, S. Kakizawa, H. N. Kingdom and S. Namba, *Mol. Plant Pathol.*, 2008, **9**, 403.
7 R. Wang, B. Bai, D. Li, J. Wang, W. Huang, Y. Wu and L. Zhao, *Mol. Plant Pathol.*, 2024, **25**, e13437.
8 F. Quaglino, Y. Zhao, P. Casati, D. Bulgari, P. A. Bianco, W. Wei and R. E. Davis, *Int. J. Syst. Evol. Microbiol.*, 2013, **63**, 2879.
9 EFSA Panel on Plant Health (PLH), *EFSA J.*, 2014, **12**, 3924.
10 J. Perumal, Y. Wang, A. Attia, U. Dinish and M. Olivo, *Nanoscale*, 2021, **13**, 553.
11 C. Baratto, G. Ambrosio, G. Faglia and M. Turina, *IEEE Sens. J.*, 2022, **22**, 23286.
12 N. Altangerel, G. Ariunbold, C. Gorman, M. Alkahtani, E. Borrego, D. Bohlmeyer, P. Hemmer, M. Kolomiets, J. Yuan and M. Scully, *Proc. Natl. Acad. Sci. U. S. A.*, 2017, **114**, 3393.

Open Access Article. Published on 20 May 2025. Downloaded on 9/10/2025 12:20:14 PM.
This article is licensed under a Creative Commons Attribution 3.0 Unported Licence.

13 L. Mandrile, S. Rotunno, L. Miozzi, A. Vaira, A. Giovannozzi, A. Rossi and E. Noris, *Anal. Chem.*, 2019, **91**, 9025.
14 L. Mandrile, C. D'Errico, F. Nuzzo, G. Barzan, S. Matic, A. Giovannozzi, A. Rossi, G. Gambino and E. Noris, *Front. Plant Sci.*, 2022, **13**, 917226.
15 S. Yeturu, P. Jentzsch, V. Ciobota, R. Guerrero, P. Garrido and L. Ramos, *Anal. Methods*, 2016, **8**, 3450.
16 V. Egging, J. Nguyen and D. Kurouski, *Anal. Chem.*, 2018, **90**, 8616.
17 C. Farber and D. Kurouski, *Anal. Chem.*, 2018, **90**, 3009.
18 C. Farber, M. Shires, K. Ong, D. Byrne and D. Kurouski, *Planta*, 2019, **250**, 1247.
19 C. Farber, R. Bryan, L. Paetzold, C. Rush and D. Kurouski, *Front. Plant Sci.*, 2020, **11**, 01300.
20 L. Sanchez, A. Ermolenkov, X. Tang, C. Tamborindeguy and D. Kurouski, *Planta*, 2020, **251**, 64.
21 L. Sanchez, A. Ermolenkov, S. Biswas, E. Septiningsih and D. Kurouski, *Front. Plant Sci.*, 2020, **11**, 573321.
22 S. Gupta, C. Huang, G. Singh, B. Park, N. Chua and R. Ram, *Sci. Rep.*, 2020, **10**, 20206.
23 G. Carminati, V. Brusa, A. Loschi, P. Ermacora and M. Martini, *Pathogens*, 2021, **10**, 811.
24 D. Ballabio and V. Consonni, *Anal. Methods*, 2013, **5**, 3790.
25 P. H. C. Eilers, *Anal. Chem.*, 2003, **75**, 3631.
26 P. H. C. Eilers, *Anal. Chem.*, 2004, **76**, 404.
27 S. Wold, A. Johansson and M. Cochi, *PLS: Partial Least Squares Projections to Latent Structures*, ESCOM Science Publishers, Leiden, 1993, pp. 523–550.
28 L. Galletto, D. Bosco and C. Marzachì, *Ann. Appl. Biol.*, 2005, **147**, 191.
29 C. Marzachì and D. Bosco, *Mol. Biotechnol.*, 2005, **30**, 117.
30 P. Margaria, M. Turina and S. Palmano, *Plant Pathol.*, 2009, **58**, 838.
31 P. Margaria and S. Palmano, *Phytoplasma: Methods and Protocols*, 2013, pp. 283–289.
32 K. Oshima, S. Kakizawa, H. Nishigawa, H. Y. Jung, W. Wei, S. Suzuki and S. Namba, *Nat. Genet.*, 2004, **36**, 27.
33 Y. Tan, Q. Li, Y. Zhao, H. Wei, J. Wang, C. J. Baker, Q. Liu and W. Wei, *PLoS One*, 2021, **16**, e0246203.
34 M. Hren, P. Nikolic, A. Rotter, A. Blejec, N. Terrier, M. Ravnikar, M. Dermastia and K. Gruden, *BMC Genom.*, 2009, **10**, 460.
35 S. Buoso, L. Pagliari, R. Musetti, M. Martini, F. Marroni, W. Schmidt and S. Santi, *BMC Genom.*, 2019, **20**, 1.
36 C. Xue, Z. Liu, L. Dai, J. Bu, M. Liu, Z. Zhao, Z. Jiang, W. Gao and J. Zhao, *Phytopathology*, 2018, **108**, 1067.
37 P. Margaria, A. Ferrandino, P. Caciagli, O. Kedrina, A. Schubert and S. Palmano, *Plant Cell Environ.*, 2014, **37**, 2183.
38 W. Wei, J. Inaba, Y. Zhao, J. D. Mowery and R. Hammond, *Int. J. Mol. Sci.*, 2022, **23**, 1810.
39 H. J. Butler, M. R. McAinsh, S. Adams and F. L. Martin, *Anal. Methods*, 2015, **7**, 4059.

This journal is © The Royal Society of Chemistry 2025